The diversity of protein turnover and abundance under nitrogen-limited steady-state conditions in Saccharomyces cerevisiae

ARTICLE *in* MOLECULAR BIOSYSTEMS · DECEMBER 2011

Impact Factor: 3.21 · DOI: 10.1039/c1mb05250k · Source: PubMed

8 AUTHORS, INCLUDING:

Pascale Daran-Lapujade
Delft University of Technology
97 PUBLICATIONS **2,266** CITATIONS
SEE PROFILE

Dick de Ridder
Delft University of Technology
139 PUBLICATIONS **3,426** CITATIONS
SEE PROFILE

Jack T Pronk
Delft University of Technology
271 PUBLICATIONS **11,312** CITATIONS
SEE PROFILE

Albert J R Heck
Utrecht University
683 PUBLICATIONS **21,733** CITATIONS
SEE PROFILE

Molecular BioSystems

Cite this: *Mol. BioSyst.*, 2011, **7**, 3316–3326

www.rsc.org/molecularbiosystems

PAPER

The diversity of protein turnover and abundance under nitrogen-limited steady-state conditions in *Saccharomyces cerevisiae*†

Andreas O. Helbig,[ab] Pascale Daran-Lapujade,[cd] Antonius J. A. van Maris,[cd] Erik A. F. de Hulster,[cd] Dick de Ridder,[def] Jack T. Pronk,[cd] Albert J. R. Heck[ab] and Monique Slijper*[ab]

Received 20th June 2011, Accepted 16th September 2011
DOI: 10.1039/c1mb05250k

To establish more advanced models of molecular dynamics within cells, protein characteristics such as turnover rate and absolute instead of relative abundance have to be analyzed. We applied a proteomics strategy to analyze protein degradation and abundance in *Saccharomyces cerevisiae*. We used steady-state chemostat cultures to ascertain well-defined growth conditions and nitrogen limited media, which allowed us to rapidly switch from ^{14}N to ^{15}N-isotope containing media and to monitor the decay of the ^{14}N mono-isotope signals in time. We acquired both protein abundance information and degradation rates of 641 proteins. Half-lives of individual proteins were very diverse under nitrogen-limited steady-state conditions, ranging from less than 30 min to over 20 h. Proteins that act as single physical complexes do not always show alike half-lives. For example the chaperonin-containing TCP-1 complex showed similar intermediate half-lives ranging from 7 to 20 h. In contrast, the ribosome exhibited a wide diversity of half-lives ranging from 2.5 to over 20 h, although their cellular abundances were rather similar. The stabilities of proteins involved in the central sugar metabolism were found to be intermediary, except for the glycolytic enzymes Hxk1p and Fba1p and the TCA-cycle proteins Lsc2p and Kgd1p, which showed half-lives of over 20 h. These data stress the need for inclusion of quantitative data of protein turn-over rates in yeast systems biology.

Introduction

To date, proteomics experiments provide a comprehensive 'snapshot' of relative protein abundances in *Saccharomyces cerevisiae*.[1,2] Much less information is gathered from such experiments about cellular protein dynamics. When comparing changes in mRNA- and corresponding protein levels, a poor correlation is often found between these two levels.[2–7] For example, Godoy *et al*. obtained a comprehensive dataset about changes in protein levels between haploid and diploid *S. cerevisiae*. Overall, the relative protein levels detected in this study showed a poor correlation with concurrent changes in mRNA levels ($R = 0.24$), which improved after correction for *e.g.* low-level microarray signals ($R = 0.46$). Only for some of the protein classes they have detected much better correlation, such as for the strong regulation of proteins involved in the pheromone response that were co-regulated at the mRNA level ($R = 0.68$). However, actual protein ratios could not be accurately predicted from mRNA levels.[2] These changes may also partly result from slight differences in growth conditions in the successive experiments, however, even for highly reproducible chemostat cultures that permit a fixed and constant specific growth rate under tightly defined nutritional conditions,[8] relatively poor correlations were detected. Kolkman *et al*. compared *S. cerevisiae* that was grown in carbon and nitrogen limited chemostat cultures, and detected a positive Spearman rank correlation of not more than 0.56 between changes in transcript and corresponding protein levels.[3] This work indicated that up-regulation in response to glucose-limitation was mainly transcriptionally controlled, whereas up-regulation in response to nitrogen-limitation was primarily controlled at the post-transcriptional level. When comparing *S. cerevisiae* aerobic and anaerobic growth conditions in chemostat cultures, also de Groot *et al*. found strong evidence

[a] *Biomolecular Mass Spectrometry and Proteomics Group, Bijvoet Center for Biomolecular Research and Utrecht Institute for Pharmaceutical Sciences, Utrecht University, Padualaan 8, 3584 CH Utrecht, The Netherlands. E-mail: m.slijper@uu.nl; Fax: +31 302533789; Tel: +31 302533789*
[b] *Netherlands Proteomics Centre, The Netherlands*
[c] *Department of Biotechnology, Delft University of Technology, Julianalaan 67, 2628 BC Delft, The Netherlands*
[d] *Kluyver Centre for Genomics of Industrial Fermentation, P.O. Box 5057, 2600 GA Delft, The Netherlands*
[e] *The Delft Bioinformatics Lab, Faculty of Electrical Engineering, Mathematics and Computer Science, Delft University of Technology, Mekelweg 4, 2628 CD Delft, The Netherlands*
[f] *Netherlands Bioinformatics Center, The Netherlands*
† Electronic supplementary information (ESI) available. See DOI: 10.1039/c1mb05250k

for post-transcriptional regulation of central cellular processes, such as glycolysis, amino-acyl tRNA synthesis and amino acid biosynthesis.[4] From these and other studies it has therefore been suggested that the regulation of cellular protein quantities not only takes place at transcriptional and translational levels, but that regulation may also occur at the level of the protein synthesis and -degradation rates, or the protein turnover rates.[3,4] Consequently, a largely missing dimension in proteomics and systems biology is a detailed insight into individual protein dynamics.

To address protein turnover, many organisms have recently been used as model, ranging from bacteria such as *E. coli*,[9] and *M. tuberculosis*,[10] to eukaryotes such as *S. cerevisiae*,[11] and mammalian cell lines like lung carcinoma cells[12] and adenocarcinoma cells,[13] but also whole animals (chicken) have been studied.[14] In the past, radioactive isotopes were employed to determine turnover rates (*e.g.* ^{3}H, ^{14}C, ^{35}S). Such methods are highly sensitive, allowing analysis of very low isotope incorporation levels using scintillation counting or autoradiography. However, to date less hazardous approaches are preferred, using mostly proteomics techniques in conjunction with incorporation of stable isotopes (^{2}H, ^{13}C, ^{14}N, ^{18}O), which allows in-depth proteome coverage. Different ways of analyzing *in vivo* protein stability have been described. Belle *et al.* used an epitope-tagged yeast strain library to determine protein half-lives. They analyzed the turnover rates of 3750 protein levels through Western blotting, using exponentially growing yeast cells, translation of which was inhibited by cycloheximide.[15] Most other reported large-scale approaches make use of a combination of 2D gel electrophoresis for protein separation and mass spectrometry to analyze turnover rates. For example, an unlabelled chase after complete ^{2}H-leucine incorporation was used to assess protein dynamics in yeast steady-state cultures.[11] For the about 50 proteins that were identified from the corresponding 2D gels, ratios of 'heavy' and 'light' labelled peptides were extracted over a time course of 50 hours and protein degradation rates were calculated using non-linear curve fitting. Gustavsson *et al.* applied time dependent incorporation of ^{15}N into the proteome of HeLa cells, separated the proteins of the samples of the time series by 2D gel electrophoresis, and analyzed ^{14}N and ^{15}N peak intensities through MS.[16] This approach has been used to evaluate the effect of heat stress on protein turnover rates, and to assess if the increase in protein levels has occurred through either *de novo* synthesis or decreased degradation rates. While for most of these studies steady-state growth conditions are assumed, Jayapal *et al.*[17] have used a double labelling method using SILAC and iTRAQ to estimate protein turnover rates in *Streptomyces coelicolor* cultures undergoing transition from exponential growth to stationary phase.

Here we present an approach that allowed us to obtain information on individual protein turnover in a high-throughput fashion. To achieve this, we used nitrogen limited *Saccharomyces cerevisiae* steady-state chemostat cultures where parameters such as density, growth rate, pH, pO and temperature can be very accurately controlled.[8] We employed a pulse-chase-like setup, switching from ^{14}N to ^{15}N-media, which permitted analysis of the protein degradation rates through the decay of the ^{14}N-labelled proteins over a time course of 16 h. We made use of multidimensional peptide separation using strong cation exchange chromatography to fractionate peptides and applied reversed phase nano-LC-MS/MS combined with label-free quantification software to align and normalize LC-MS data from six different sampling time points. This enabled us to obtain turnover and half-life values for about 650 proteins. Additionally, using label-free quantification allowed us to estimate the cellular expression levels for these proteins. We show that this information about protein level and turnover rate provides a complementary viewpoint compared to relative protein quantification, and allows us to assess protein families such as chaperones, metabolic pathways like the central sugar metabolism, and large protein complexes such as the ribosome. The data represent a major inventory of protein degradation rates, demonstrating that this approach is very suitable for acquiring information on temporal protein dynamics in a straightforward and comprehensive manner.

Results

Experimental design

The large-scale analysis of protein turnover rates is a significant challenge, getting so far somewhat less attention in the proteomics field. Here we present an analysis strategy that allowed us to obtain information on protein degradation in wild type *S. cerevisiae*. As illustrated in Fig. 1, S. *cerevisiae* was grown in a chemostat under nitrogen-limited conditions (using ^{14}N ammonium sulfate) until a steady-state culture was established. Then, the medium reservoir was replaced for a vessel in which ^{14}N ammonium sulfate was exchanged for ^{15}N ammonium sulfate. This resulted in a time-dependent incorporation

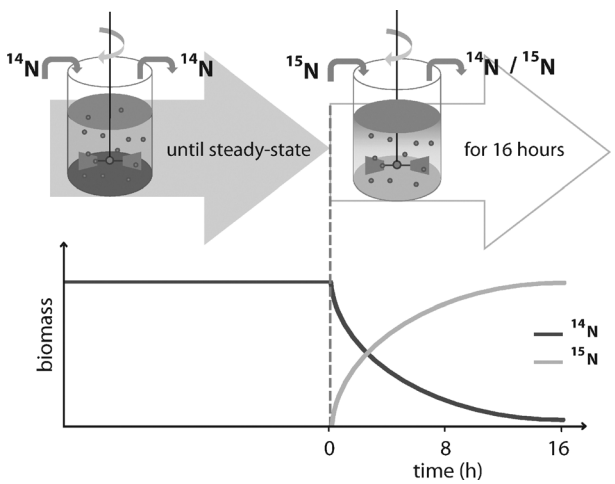

Fig. 1 Schematic overview of cell culture and time dependent stable isotope incorporation. *S. cerevisiae* was grown in chemostats under nitrogen limitation with a continuous supply of ^{14}N medium until steady-state was obtained. At steady-state, the medium supply was switched to ^{15}N and the culture was grown for another 16 hours. During steady-state culturing, the growth rate was kept constant at 0.1014 h^{-1} throughout the experiment, and therefore total yeast biomass in the fermenter remained also constant. Newly synthesized proteins incorporated increasing amounts of the ^{15}N-stable isotope over time, therefore a simultaneous one-phase decay of the proteins containing the ^{14}N isotope can be detected.

of ^{15}N stable isotopes into all cellular proteins. A schematic experimental overview is given in Fig. S1 (ESI†). One sample was taken just prior to the initiation of the ^{15}N feed, and further sampling occurred in five distinct intervals after 2, 4.5, 7, 10, and 16 h. Care was taken to prevent disruption of the steady-state growth by taking small sample volumes.

Corresponding ^{14}N mono-isotopic peptide peaks of MS^1 spectra from samples of six different sampling time points were collected. Database searches using MASCOT were performed to identify the proteins. The normalized ^{14}N mono-isotopic peptide peak intensities were summed up for each protein. Only summarized protein peak intensities that could be detected for all six samples were used as input to calculate the turnover rates.

The gradual incorporation of the ^{15}N stable isotope into yeast proteins led to quite complex peptide isotope peak distributions, although the spectra are well-resolved. Examples are shown in Fig. 2A, in which the ^{14}N mono-isotopic peak is highlighted with a white-headed arrow, and the ^{15}N mono-isotopic peak of the fully ^{15}N-labelled peptide with a black-headed arrow. It is apparent from the spectra in Fig. 2A that many of the newly synthesized proteins have only partially incorporated the ^{15}N isotope. Since we used nitrogen-limited growth conditions, we could assume that the ^{14}N-ammonium sulfate supply in the fermenter was immediately exchanged for the ^{15}N-ammonium sulfate supply. The exchange of nitrogen isotopes may, however, be somewhat slower within the yeast biomass, *e.g.* as a result of recycling of ^{14}N amino acids. Further, we could assume that the ammonium sulfate import rate into the *S. cerevisiae* cells was not affected by the change in nitrogen isotope supply. From earlier experiments in steady-state chemostat cultures grown on ^{14}N or ^{15}N-media aimed at relative protein quantification, no significant effect was detected, as duplicate isotope-reversed experiments (with reversed ^{14}N and ^{15}N-media) resulted in extremely similar quantitative data sets.[3,4]

The aim of our strategy was to obtain the mono-isotopic ^{14}N peak intensity of each peptide for all six sampling time points. Due to the use of a chemostat culture, the cells displayed a constant growth rate and the reservoir medium contained a constant chemical composition, consequently, the total biomass in the cultures remained constant throughout the experiment. Therefore, for each peptide, the sum of all isotope peak intensities (*i.e.* all ^{14}N-labeled peptide peaks, all $^{14}N/^{15}N$-labeled peptide peaks, and all ^{15}N-labelled peptide peaks; Fig. 2A) was considered to be constant throughout the six corresponding spectra. Using this rationale, we utilized the 'visual script' option in the Rosetta elucidator software to normalize the ^{14}N mono-isotopic peak intensities. These normalized ^{14}N mono-isotopic peak intensities were used as input to calculate both the *S. cerevisiae* protein abundances and the corresponding turnover rates.

Protein turnover rates and half-lives

The Mascot search leads to the identification of 9431 unique peptides that could be traced throughout all six time points, which corresponds to 1230 unique proteins. First, we calculated protein degradation rates from the exponential decay of

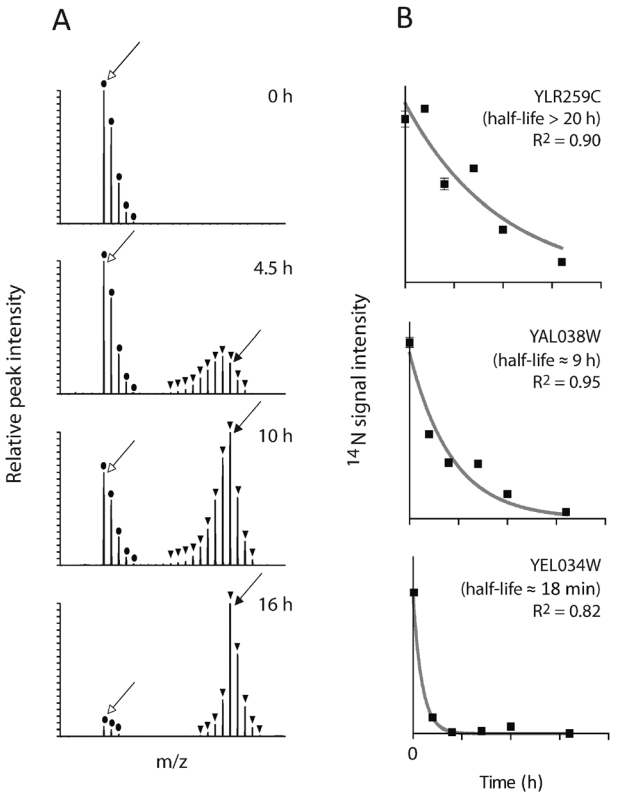

Fig. 2 Protein turnover analysis using non-linear curve fitting, assuming first order kinetics. (A) Examples of the evolution of a peptide peak isotope distribution during the 16-hour gradual incorporation of the ^{15}N isotope. The ^{14}N mono-isotopic peak is indicated with a white-headed arrow, and the ^{15}N mono-isotopic peak with a black-headed arrow. Further, the ^{14}N-labeled peptide peaks are labelled with circles and the (partially) ^{15}N-labelled peptide peaks with triangles. Many partially ^{15}N-labeled peaks can be observed for the peptides of lysates from the sampling time points of 4.5, 10 and 16 h. For protein turnover analysis, the decrease in time of the sum of its normalized ^{14}N mono-isotopic peptide peak intensities was monitored. (B) Typical results of one-phase decay curve fitting by using normalized and summed ^{14}N mono-isotopic peptide peak intensities for three proteins with notably different protein turnover rates. YLR259C displays a markedly stable behaviour (half-life is close to the dilution rate), YAL038W appears to be a protein of intermediary stability, while YEL034W shows very fast degradation.

the summarized ^{14}N mono-isotopic peptide peak intensities for each protein, which is given by the following equation (assuming first order kinetics):

$$IA_{14}(t) = IA_{14}(0) \times e^{-[t(K_{Deg}+D)]}$$

IA_{14} = isotope abundance or ^{14}N mono-isotopic peak intensity (*i.e.* for each protein the sum of the detected and normalized peptide ^{14}N mono-isotopic peak intensities); K_{Deg} = protein degradation rate; D = dilution rate (= 0.1014 h^{-1})

This allowed for subsequent calculation of protein half-life values:

$$t_{1/2} = \ln 2/K_{Deg}$$

where $t_{1/2}$ = half-life (in h).

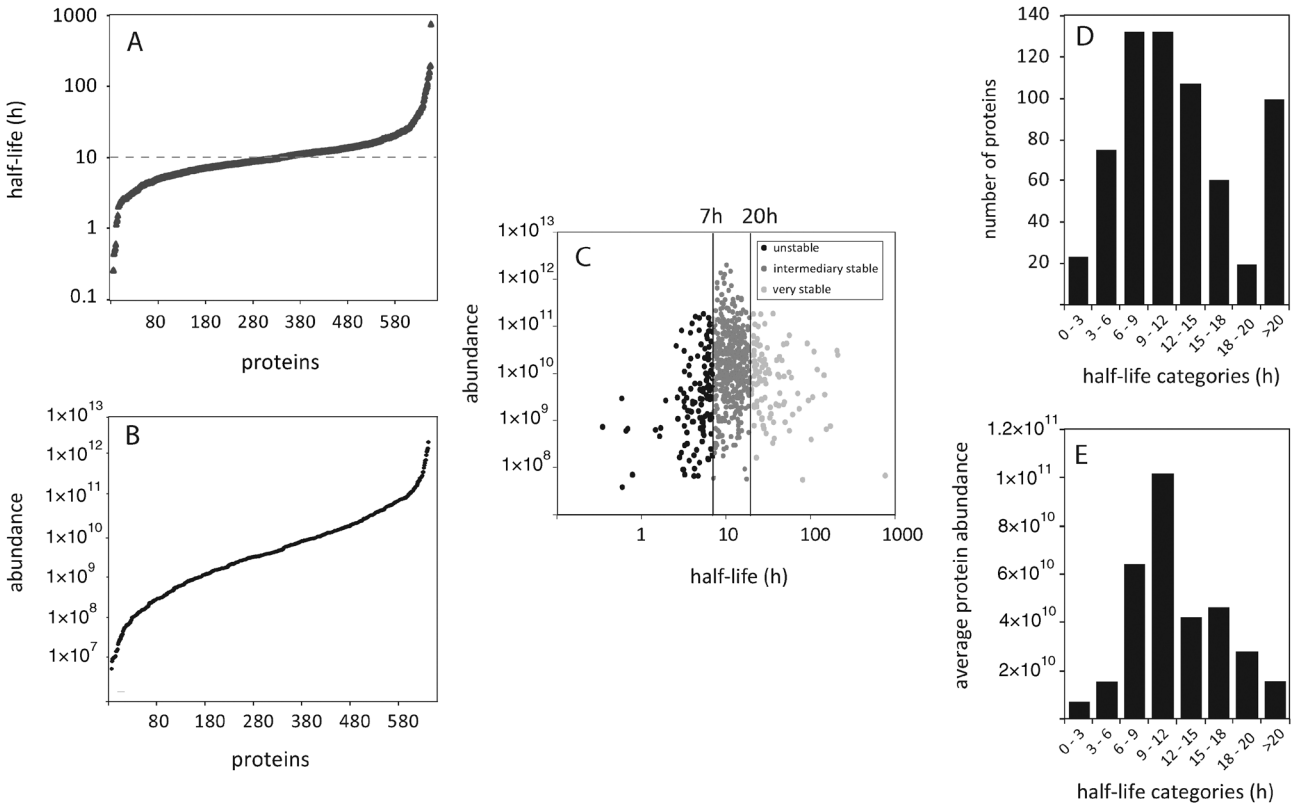

Fig. 3 Overview of protein turnover and abundance in *S. cerevisiae* under nitrogen-limited steady-state conditions. (A) Plot of the half-lives of all 641 proteins, the median value is indicated by a dotted line at 10.8 h. (B) Abundance range of all 641 proteins, based on total ion intensity (as described in the 'methods' section). (C) Distribution plot of protein half-lives *versus* their abundance, showing their poor correlation. The half-life thresholds that we defined for very stable ($t_{1/2} > 20$ h) and unstable ($t_{1/2} < 7$ h) proteins are indicated in the plot. (D) Binned categories of protein half-lives, showing how many proteins were detected within each category. (E) Binned categories of protein abundances, showing how many proteins were detected within each of these categories.

Data normalization

We applied stringent data analysis criteria, demanding that peptide ion intensities were obtained for the samples of all 6 sampling time points. We further used a cut-off value for R^2 of 0.6, resulting in a list of 641 proteins for which the turnover rates and thus half-lives could be calculated (Table S1, ESI†). It should be noted that if degradation rates are approaching the dilution rate, calculation of half-lives become much less reliable, mostly for very stable proteins with half-lives of approximately over 20 h.

Fig. 2B illustrates the decay of the normalized ^{14}N mono-isotopic peak intensity for three proteins that show clear differences in protein turnover rates. YLR259C exhibits a relatively stable behaviour with a half-life of >20 h, and YAL038W has a shorter half-life of 9 h, while YEL034W illustrates a much faster protein turnover with a half-life of 18 min. Fig. 3 shows the plots of the 641 protein half-lives (A). The median of the calculated half-lives was 10.8 h, and the large majority of the proteins (405 proteins) showed intermediate half-lives between 7 and 20 h (Table S2, ESI†). To guide further discussions, we subjectively defined the 137 proteins with a shorter half-life than 7 h as 'unstable' proteins, the 99 proteins with a half-life longer than 20 h as 'very stable' proteins, and the 405 proteins with the half-lives between 7 and 20 h as 'intermediary' stable proteins.

Protein abundance

Another important aspect of the cellular proteome is the actual protein abundance. Using the Rosetta software, we summed the normalized peptide ^{14}N-mono-isotopic peak intensities for each confidently identified protein. To do this, we considered the sample obtained at time point 0 h (*i.e.* just before the switch to ^{15}N-media) as a measure for initial protein abundance. It has been previously shown that such ion intensities can be regarded as a reasonable estimate for protein abundance.[18–20] From our experiments we concluded that these quantitative data correlated well with those obtained by spectral counting, which is another method to assess protein abundance (data not shown).[18,21] In Fig. 3B the protein abundances are plotted for all 641 proteins (data summarized in Table S1, ESI†). It can be observed from this plot that the protein abundances span about 5 orders of magnitude, indicating that our methodology allowed us to estimate protein turnover rates from a wide range of cellular protein concentrations. The observed turnover rates do however not correlate well with protein abundance, as can be concluded from Fig. 3C. This may be due to the fact that the size of this dataset is limited. We calculated reliable turnover rates of 641 *S. cerevisiae* proteins, while Schwanhäusser *et al.*[22] calculated turnover rates for over 5000 proteins in mouse fibroblast cells. They detected that in general abundant

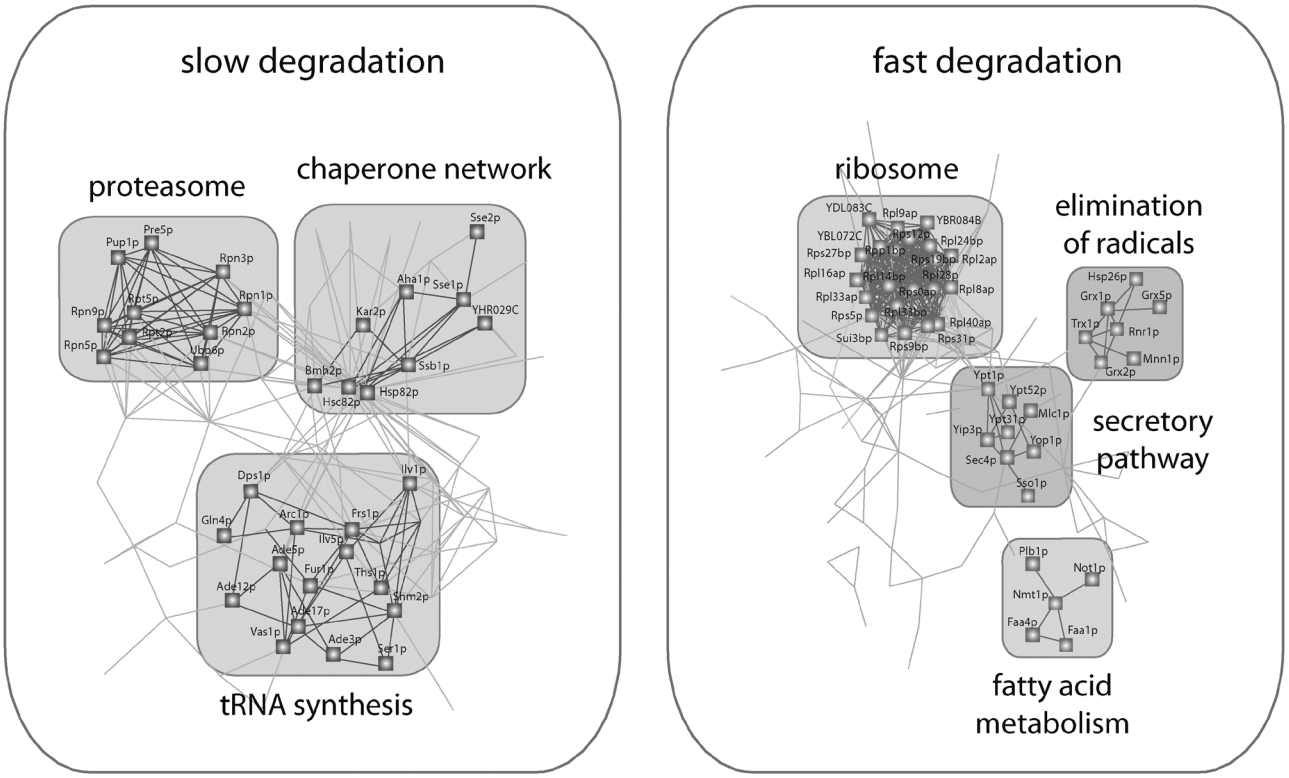

Fig. 4 Protein networks of stable and unstable proteins (data from Table S1 (ESI†)). Subsets of the very stable proteins (99 proteins, $t_{1/2}$ > 20 hours) and unstable proteins (137 proteins, $t_{1/2}$ < 7 hours) were separately analyzed for their protein interaction networks using STRING.[23] The most prominent protein interaction clusters as classified by STRING are highlighted in the map.

proteins are significantly more stable than less abundant ones, and additionally, that these proteins are significantly shorter. We categorized the protein half-lives into intervals of 3 h (in the range 0–20 h), and one interval of >20 h (Fig. 3D). When comparing the same half-life categories against the average protein abundances per category (Fig. 3E), we observed that the half-life category containing the largest number of proteins (Fig. 3D) is the same as the one displaying proteins with the highest abundance, thereby indicating a bias of our analysis towards abundant proteins.

Protein network analysis

We performed gene ontology and protein network analysis on protein half-life data using the network analysis tool STRING,[23] to find networks of proteins that might be related to the two categories of extreme protein half-lives. For this purpose we considered again the subset of our data that contained all very stable proteins ($t_{1/2}$ > 20 h; 99 proteins), and the part that contained the unstable proteins ($t_{1/2}$ < 7 h; 137 proteins). Fig. 4 shows the retrieved protein interaction maps of these very stable and unstable subsets. The map of very stable proteins shows interaction clusters for 10 of the 28 known 20S proteasome proteins, for 9 chaperones and for 15 proteins involved in tRNA synthesis (data extracted from Table S1, ESI†). In the category of unstable proteins, significant protein interaction clusters were found for 20 of the 78 ribosomal proteins, for proteins involved in the secretory pathway, in fatty acid biosynthesis and in free radical scavenging. It was not surprising to observe that proteins such as glutaredoxin (Grx1p, -2p and -5p) or thioredoxin I (Trx1p), which are heavily exposed to reactive oxygen species and directly interact with them, have short half-lives. These proteins are prone to oxidative damage and therefore need a fast turn-over to protect cells against oxidative stress. Most identified proteins involved in the protection against oxidative stress had short half-lives, a few had average half-lives (for instance the two superoxide dismutase iso-enzymes Sod1p and Sod2p), but none were identified with long half-lives. Our data show that the extreme half-life categories of proteins ($t_{1/2}$ < 7 h or $t_{1/2}$ > 20 h) contain only parts of known protein networks such as a subset of proteins from the ribosomes, of the proteasome or a subset of proteins involved in *e.g.* free radical scavenging, suggesting that these cellular functions basically do not require proteins that all display extremely short or long half-lives.

Discussion

Benefits of label-free quantification

Recently, label-free quantification software has been developed for protein quantification by mass spectrometry. This label-free methodology relies on the alignment of the corresponding mono-isotopic MS[1] peptide peaks from multiple LC-MS experiments *via* accurate mass and retention time, and allows protein quantification based on peptide peak intensities from separate chromatographic experiments.[24,25] The advantage of this approach is that the quantification is uncoupled from peptide identification, as it is performed on

MS^1 peaks prior to the peptide identification using database searches,[26] thus also for the ^{14}N mono-isotope peaks that show low intensities (*i.e.* from samples collected in the late time points) that were not selected for MS^2. After alignment of the corresponding MS^1 peaks from all LC-MS runs, peptide identifications from the first experiment ($t = 0$ h) were used across all aligned data sets. To calculate turnover rates, we analyzed the decay of the protein ^{14}N mono-isotopic peak intensities (*i.e.* sum of its peptide ^{14}N mono-isotopic peak intensities) assuming first order kinetics. Using our approach with label-free quantification we could reliably estimate half-lives and protein abundances of 641 yeast proteins.

The current experiment has been performed under nitrogen-limitation, a condition in which the residual nitrogen (in the form of ammonium sulfate) is extremely low (below 0.02 mmol nitrogen L^{-1}). This low concentration of nitrogen in the culture enables the rapid replacement of ^{14}N by ^{15}N-labelled ammonium sulfate following the label-switch. Although more challenging, the same labelling experiment can be performed with other nutrient limitations such as carbon or sulfur limitation. Under limitations other than nitrogen, the residual nitrogen concentration is higher, but can be adjusted as to become very low while remaining non-limiting.[27,28] Furthermore, conversely to previously published work,[29] this method does not require the use of mutant strains and can be performed in well-controlled synthetic media.

Comparison with similar protein turnover studies

We compared our results with the study of Pratt *et al.*,[11] who also used chemostat cultures to obtain proteome data on the turnover of *S. cerevisiae* proteins. Pratt *et al.* reported turnover rates on 50 proteins, for 23 of which we also obtained values. Some of the turnover rate values were quite similar, *e.g.* for Hsp26p we detected a turnover rate of 0.129 (h^{-1}) *versus* Pratt *et al.* 0.126 (h^{-1}). For Tpi1p, the detected turnover rates were 0.077 (h^{-1}) *versus* 0.097 (h^{-1}), and for Ssa1p these were 0.88 *versus* 0.103 (h^{-1}), respectively. In contrast, for very stable proteins in our dataset, such as Kar2p, we detected a turnover rate of 0.018 (h^{-1}) whereas Pratt *et al.* reported a value of 0.095 (h^{-1}), corresponding to a five-fold difference in turnover rates. Averaged over all 23 proteins the correlation coefficient between the two datasets was only −0.011. A potential limitation in the dataset of Pratt *et al.* arises from their 2D gel approach, wherein a single spot can contain multiple proteins, thereby making it difficult to accurately estimate turnover rates of individual proteins.[11] Another factor that may contribute to the poor correlation between the two datasets is that Pratt *et al.* used a leucine auxotrophic *S. cerevisiae* strain, grown under glucose limitation, while our experiments were performed with a prototrophic *S. cerevisiae* strain grown under nitrogen limitation. It is very well conceivable that turnover rates of individual proteins are affected by cultivation conditions and, perhaps, may also be yeast strain dependent. In the fast developing field of quantitative proteomics, it is important to regularly perform inter-laboratory comparisons and evaluations of alternative procedures. We propose that the nitrogen limitation cultivation regime described in the present study offers a useful reference for such community efforts.

Turnover rates of proteins within known complexes

How similar are turnover rates of proteins within known functional complexes? Chaperone-assisted folding by the CCT complex (chaperonin containing TCP-1) has been shown to occur while proteins are being synthesized.[30] CCT is a 900 kDa multi-subunit complex that has a critical function in protein folding of a small number of cellular proteins, like proteins of the actin and tubulin families, histone deacetylases and cell cycle regulators.[31] The detected proteins of this CCT chaperone complex show largely similar protein half-lives for the subunits Cct2p, Cct3p, Cct4p, Cct7p, Cct8p and Tcp1p. We consider this consistent with the formation of a stable, functional chaperone complex of which the subunits show hardly any exchange (Table S2, ESI†). Conversely, the subunits within the ribosome displayed a wide range of half-lives. The ribosome is one of the most abundant protein complexes in the cellular cytoplasm and is involved in protein translation. The *S. cerevisiae* ribosome consists of 78 proteins (of which 59 are duplicated), 32 of the small subunit and 46 of the large subunit, and four ribosomal RNAs.[32,33] Ribosome assembly is a very complex process that starts with the association of ribosomal proteins with rRNAs within the nucleolus. Separate ribosomal subunits are subsequently transported from the nucleolus to the cytoplasm, after which they assemble into mature ribosomes. Ribosomal biosynthesis is tightly controlled and connected to other major cellular pathways such as protein processing and protein folding.[34] In this study, we calculated turnover rates and abundance values for 67 ribosomal proteins, of which 33 of the 60S large ribosomal subunit, 31 of the 40S small subunit, and 3 of the ribosomal stalk (Fig. 5; Table S1 (ESI†)). As expected, the abundances of

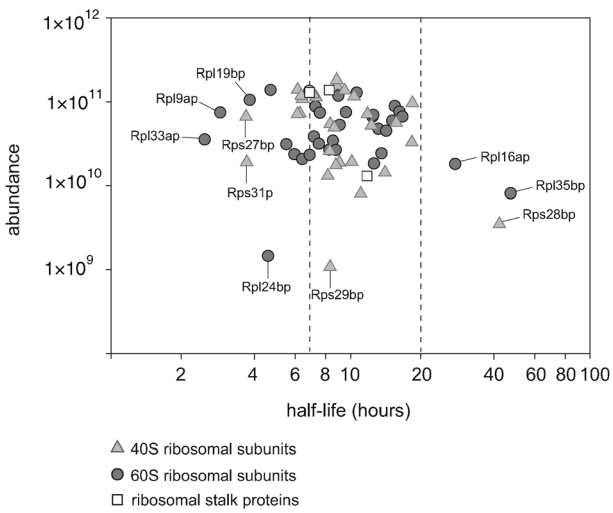

Fig. 5 Protein turnover and abundance of ribosomal proteins. Protein half-lives *versus* abundance for the 67 detected 40S (grey triangles), 60S (dark grey circles) ribosomal subunits, and the ribosomal stalk proteins (white squares). Protein half-lives are indicated on the *x*-axis, while corresponding protein abundances are indicated on the *y*-axis. Protein names are only indicated if proteins showed relatively exceptional behaviour regarding their half-life. The box (dashed lines) indicates the majority of ribosomal complex members that show abundances within two orders of magnitude and intermediate protein half-lives (7–20 h).

the majority of ribosomal proteins were found to be similar, with very few exceptions (Rps28Bp, Rps29Bp and Rpl24Bp), which may be reflected by a low stoichiometric representation within the complex.[35] Our data show that the *S. cerevisiae* ribosomal proteins exhibit half-lives that range from 2.9 (for Rpl9Ap) to 46.9 h (for Rpl35Bp). In total, 20 ribosomal proteins show half-lives shorter than 7 h of which 11 of the 60S and 9 of the 40S ribosomal subunit (Fig. 5). Of these, the ribosomal proteins Rpl33Ap, Rpl9Ap, Rpl19Bp, Rps27Bp, and Rps31p display much faster turnover rates (half-lives between 2.5 and 4 h). Only three proteins, Rps28Bp, Rpl16Ap and Rpl35Bp, show half-lives longer than 20 h. This wide variety in half-lives for subunits within functional protein complexes may be explained by the fact that some subunits fulfill concurrently other functions within the cell. For example the protein Rps31p is also involved in translational regulation *via* eIF2B,[36] which might explain its atypical degradation rate. Other known functions of ribosomal subunits are auto-regulation of the protein- and RNA synthesis of the ribosomal subunits themselves, and also regulation of mRNA splicing and mRNA half-lives.[37] Further, it has been suggested earlier for rat ribosomal proteins that ribosomes are not synthesized and degraded as functional units, but instead that most ribosomal proteins are rapidly exchanged with proteins present in the cytoplasm.[38] Recently Schwanhäusser *et al.*[22] analyzed protein turnover rates for cultured mouse fibroblast cells and they also detected a wide variety in ribosomal protein half-lives, ranging from 11.23 h for the Rps27A ribosomal protein to 271.11 h for Rps15 (Table S3, ESI†). No correlation exists between these two data sets, which may be expected for such diverse models.

Like the protein turnover data of mouse fibroblast cells[22] our data indicate that protein half-lives show a wide variety, even if proteins are organized in physical protein complexes, which would suggest that these entities can be affected significantly by dynamics such as subunit exchange.

Protein chaperone families

Also proteins with similar functions, like within the chaperone protein families, do not always exhibit related turnover rates. Table S2 (ESI†) shows turnover rates of the HSP60, HSP70 and HSP90 chaperone protein families. The chaperone proteins Hsc82p and Hsp82p of the HSP90 family contribute to fold a specific subset of proteins into their native conformation and are both very stable (Table S2, ESI†).[39] Both proteins show a sequence homology of 97% and demonstrate similar cellular levels according to our data. This is in contrast to the findings of Borkovich *et al.* who described that Hsp82p levels are strongly increased during heat stress, while Hsc82p is usually present at high protein levels.[40] The HSP90 co-chaperone Sgt1p has been shown to interact with other HSP90 proteins but also functions as a dimeric interactor of Skp1p and is known to be involved in the assembly of the centromere–DNA binding complex.[41,42] In contrast to other proteins of this HSP90 protein family, this Sgt1p protein showed fast turnover ($t_{1/2} \approx 0.6$ hours).

Cyclophilins are proteins that belong to a protein family of *cis–trans* peptidyl propyl isomerases. Cpr1p, however, seems to perform multiple other functions that deviate from mammals to yeast.[43] This protein becomes essential for the cell only if the function of Ess1p is impaired. This isomerase binds to phosphorylated protein stretches, resulting in change of conformation of its target proteins.[43] Additionally, it has been proposed that Cpr1p is involved in regulatory processes within the nucleus that affect meiosis and sporulation.[44] Another protein of the same cyclophilin protein family, Cpr3p, is involved in protein folding within the mitochondria.[45] This diversity in function and cellular localization may account for the detected differences in protein turnover, since we found a half-life of approximately 10 h for Cpr3p and of larger than 20 h for Cpr1p (Table S2, ESI†).

Other detected molecular chaperone systems are proteins belonging to the SSA HSP70 protein family (Ssa1p, Ssa2p and Ssa3p) or to the SSE HSP70 protein family, which also assist in protein folding and prevent protein aggregation. These proteins are characterized by their ATP dependent stabilization of substrates.[46,47] Proteins belonging to the SSA protein family show very high sequence homology and were all found to display similar half-lives between 7 and 11 hours (Table S2, ESI†). In contrast, the SSE (also HSP110) protein family exhibits a different function and acts mainly as nucleotide exchange factor for the SSA chaperones[48] (*i.e.* removal of ADP after ATP hydrolysis), which may explain their very stable half-lives of over 20 h (the half-life of Sse1p is 24.5 h, and that of Sse2p is 32.9 h, respectively; Table S2 (ESI†)).

The central carbon metabolism

In *S. cerevisiae*, glucose metabolism is initiated by the well-known cytosolic reactions of the glycolysis. Pyruvate formed in glycolysis can be further metabolized by ethanol fermentation *via* multiple isoenzymes of pyruvate decarboxylase and NAD^+-dependent alcohol dehydrogenases.[49,50] Alternatively, oxidative decarboxylation of pyruvate by the mitochondrial pyruvate dehydrogenase complex can yield acetyl-CoA, which can be oxidized *via* the tricarboxylic acid (TCA) cycle. Cellular abundances of enzymes active in this core metabolic machinery of the yeast cell differed by approximately four orders of magnitude (Fig. 6A; Table S1 (ESI†)). As illustrated in Fig. 6A, most enzymes from TCA- and glyoxylate cycle showed markedly lower levels than enzymes involved in glycolysis, which is consistent with glucose repression of the former two pathways.[51] Similar observations were also made by Picotti *et al.*, who quantified these proteins using selected reaction monitoring mass spectrometry of yeast proteins.[1] Most glycolytic proteins were also found to be in the highest abundance range in the studies of Ghaemmaghami *et al.*,[52] and also, the TCA- and glyoxylate cycle proteins showed an overall lower abundance. They analysed the global protein expression in a totally different way, namely by Western blotting on tagged proteins. In contrast to our experimental setup, Ghaemmaghami *et al.*[52] tagged the proteins, and also, they used cycloheximide to stop protein synthesis. Further, different *S. cerevisiae* strains have been used in these studies (lab strain transfected with genes encoding tagged proteins *versus* wild type strain), together with different growth conditions (*e.g.* shake flasks *versus* chemostat cultures, and synthetic

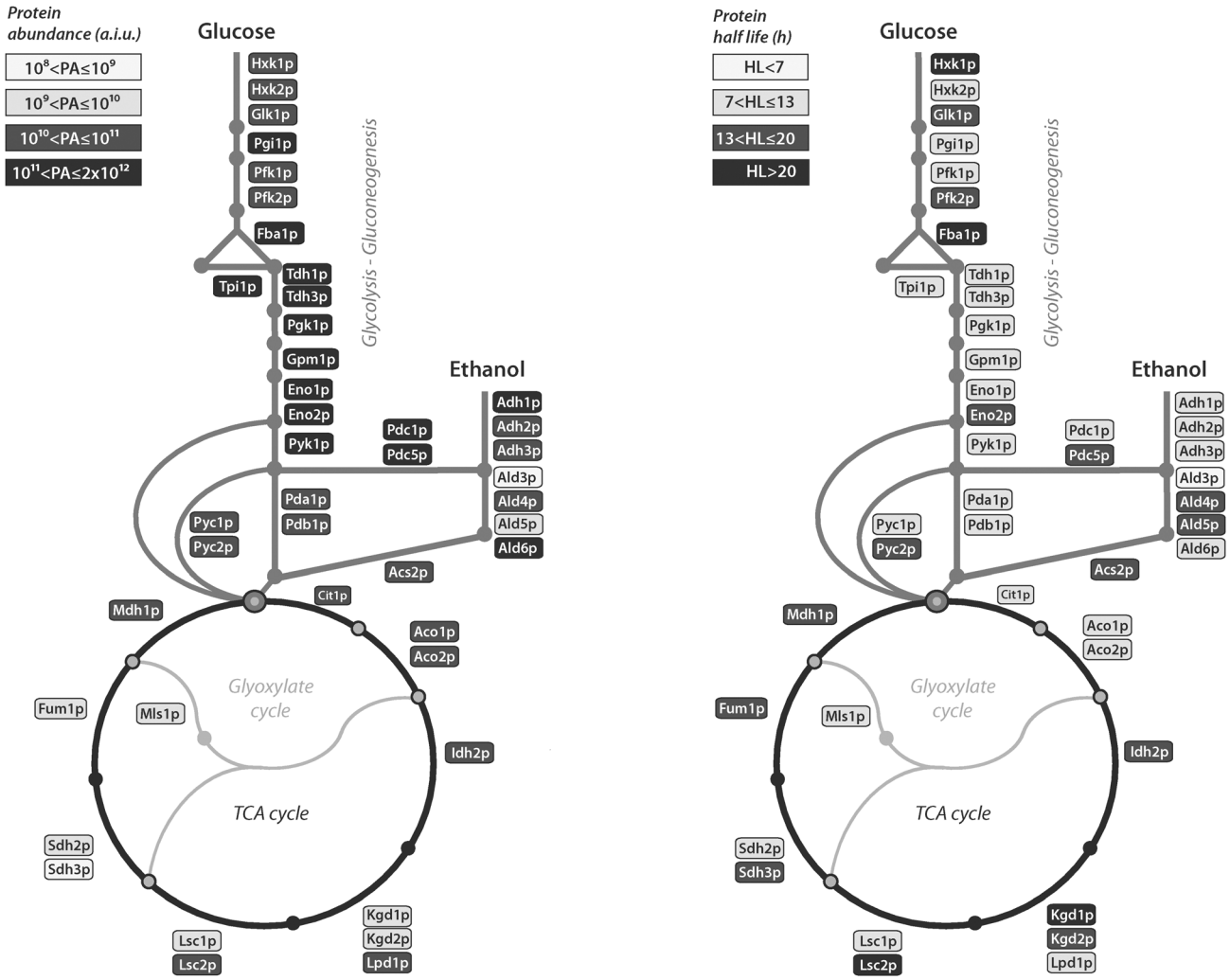

Fig. 6 Protein abundance and half-lives of enzymes of the central carbon metabolism. A pathway map indicating the enzymatic steps involved in the central sugar metabolism (glycolysis, TCA-cycle, glyoxylate cycle and alcohol fermentation) of *S. cerevisiae*. Dots are indicative for metabolites while only glucose and ethanol are highlighted in the map. For each metabolic step, only those enzymes are indicated for which the turnover rates could be detected. (A) Displays the metabolic pathway map indicating enzyme abundances (indicated in the legend as different categories of arbitrary intensity units; a.i.u.). In general, the glycolytic enzymes are more abundant than the other enzymes. (B) The same pathway map as under (A), indicating enzyme half-lives. Again, the legend with half-life categories as indicated with different grey tones is displayed at the left side of part B. Only a few enzymes, Hxk1p, Fba1p, Lsc1p and Kgd1p, are very stable.

versus complex media), which may all account for the observed differences in protein abundances.[52] For example, Costenoble *et al.*[53] compared the *S. cerevisiae* proteome for five growth conditions, amongst which synthetic media *versus* complex media, and found drastic changes in protein abundances for these two different conditions.

Most of the proteins involved in central carbon metabolism exhibited in our study an intermediate half-life of 7 to 20 h (Fig. 6B; Table S1 (ESI†)). This may represent an evolutionary compromise between energy cost of protein synthesis and metabolic flexibility: upon a cessation of synthesis (*e.g.* by transcriptional down-regulation of the structural gene), extremely stable proteins will only be diluted slowly by cell division.

Exceptions on these intermediate half-lives were detected for Ald3p, which is an unstable protein that exhibited a relatively small half-life of 5.9 h, and for three very stable proteins with a half-life of over 20 h, which are Hxk1p, Lsc2p and Kgd1p (Table S1 (ESI†); note that we indicated that half-lives > 20 h could not be calculated very reliably, as the degradation rate is then extremely close to the dilution rate). Hexokinase 1 is one of three iso-enzymes (Hxk1p, Hxk2p, and Glk1p) that catalyse the first, rate-limiting step in the glycolysis, *i.e.* the phosphorylation of glucose.[54] Obviously, while hexokinase 1 is the most stable of these three enzymes in our experiments ($t_{1/2}$ > 20 h; Table S1 (ESI†)), Belle *et al.*[15] found a markedly lower half-life value for Hxk1p ($t_{1/2}$ = 0.8 h), and a relatively higher half-life value for Glk1p ($t_{1/2}$ = 2.3 h), while no value for Hxk2p was reported. Again, like for the cellular protein abundances, half-life values may also be hard to compare between different strains and growth conditions.

Other very stable proteins are found in the TCA cycle, *i.e.* Lsc2p, part of the succinyl-CoA ligase complex, and Kgd1p, part of the α-ketoglutarate dehydrogenase complexes. A functionally active succinyl-CoA ligase complex consists of two

subunits, namely Lsc1p and Lsc2p.[55,56] The observation that Lsc1p shows an intermediary half-life of only 11 h is a further illustration that, apparently, proteins active within a single functional complex can show different protein dynamics.

Yeast glycolytic proteins represent a sizable fraction of the total cell protein (up to 21% of the total cellular proteins),[57] and, under some cultivation conditions, their synthesis may represent a significant energetic burden.[58] Quantitative information on the *in vivo* turnover rates of these and other highly expressed yeast proteins is essential for an accurate estimate of the real ATP costs of protein turnover in growing microbial cultures and, thereby, for the relative contribution of this process to maintenance of growing and non-growing cultures.

For the central carbon metabolism our data show altogether that the cellular glycolytic enzyme levels are one or two orders higher than most enzyme levels of the TCA- and glyoxylate cycle, and also, that over 90% of the detected central carbon metabolism proteins show intermediate half-lives.

Experimental

Cell culture and sample preparation

The laboratory strain *Saccharomyces cerevisiae* CEN.PK113-7D (*MAT*a) was grown at 30 °C in 2 L chemostats as described earlier.[3,59,60] Cultures were supplied with a defined mineral medium as described by Kolkman *et al.*[3] that limited growth by nitrogen, the sole source of which was ^{14}N ammonium sulfate, with all other growth requirements in excess. The dilution rate (which is equivalent to growth rate in steady-state cultures) was set at 0.1014 h^{-1}; the pH was measured online and kept constant at 5.0 by the automatic addition of 2 M KOH with the use of an Applikon ADI 1030 biocontroller. Stirrer speed was maintained at 800 rpm and the gas inflow was 0.5 L min^{-1}. Dissolved oxygen was measured online with an oxygen electrode (Ingold model 34 100 3002), and was above 60% of air saturation. After steady-state growth was accomplished, the ^{14}N ammonium sulfate medium supply was exchanged for medium containing ^{15}N ammonium sulfate for a 16-hour time course.

Samples were taken directly from the chemostat, using special small sampling ports that enable small sample sizes with very short residence time, to minimize interruption of the steady-state growth. Samples were taken at 0 hours (*i.e.* just before the ^{15}N switch), and after the switch to ^{15}N media at 2 hours, 4.5 hours, 7 hours, 10 hours and 16 hours. The cells were washed in ice cold water, and snap-frozen in liquid nitrogen to prevent unwanted protein synthesis and degradation after harvest. Yeast cells were lyophilized prior to protein extraction. Samples of 10 mg lyophilized yeast cells were resuspended in 200 μL of a solution containing 4% SDS, 25% glycerol, and 138 mM TRIS pH 6.8 and 200 mM DTT. The suspension was kept on ice and after the addition of glass beads it was vortexed 5 times for 5 min to break the cells and to solubilize the proteins. The supernatant was then centrifuged at 3000 *g* for 5 min to remove non-solubilized material. The protein sample was then embedded within polyacrylamide through the addition of 12% acrylamide, 0.5% TEMED and 5 μL of 10% ammonium persulfate. The resulting gel matrix was cut into small pieces, fixed (30% methanol, 20% acetic acid), and washed extensively with 50 mM ammonium bicarbonate to remove detergent and other contaminating agents. Reduction and alkylation were carried out as previously described for in-gel digestion.[61] After overnight digestion with trypsin, peptides were extracted from the gel by the addition of 100% acetonitrile which was removed from the sample by vacuum evaporation.

Strong cation exchange chromatography

Yeast sample peptides were further separated using strong cation exchange chromatography.[62] For each time point separately, peptides corresponding to 1 mg of protein material were loaded onto two C18 cartridges using an Agilent 1100 HPLC system. The applied flow rate was 100 μL min^{-1} using H_2O, pH 2.7, as eluent. After that peptides were eluted from the trapping cartridges with 80% acetonitrile, pH 2.7, onto a PolySulfoethyl A column 200 × 2.1 mm (PolyLC inc.) for 10 min at the same flow rate. Separation of differently charged peptide populations was performed using a non-linear gradient, *i.e.* from 0 to 10 min 100% Eluent A (5 mM KH_2PO_4, 30% acetonitrile, pH 2.7), from 10 to 15 min a linear increase to 26% Eluent B (5 mM KH_2PO_4, 30% acetonitrile, 350 mM KCl, pH 2.7), from 15 to 40 min a linear increase to 35% Solvent B, and from 40 to 45 min to 60% Eluent B. At 49 min the concentration of Eluent B was 100%. The column was subsequently washed for 6 min with Eluent B and finally equilibrated with 100% Eluent A for 9 min. The flow rate was 200 μL min^{-1}. From the start of the run, approximately 40 fractions were collected in 1 min intervals. After evaporation of the solvents, the five peptide fractions containing the majority of the +2-charged peptides[62] were analysed by reversed phase LC-MS/MS for each time point of harvest.

Mass spectrometry

The MS-analysis was performed using a nano LC-LTQ-Orbitrap (Thermo, San Jose, CA). An Agilent 1200 series LC system was equipped with a 20 mm Aqua C18 (Phenomenex, Torrance, CA) trapping column (packed in-house, id, 100 μm; resin, 5 μm) and a 400 mm ReproSil-Pur C18-AQ (Dr Maisch GmbH, Ammerbuch, Germany) analytical column (packed in-house, id 50 μm; resin, 3 μm). Trapping was performed at 5 μL min^{-1} for 10 min with Eluent A (0.1 M acetic acid in water), and elution was achieved with a gradient of 10–35% B (0.1 M acetic acid in 80/20 acetonitrile/water) in 90 minutes for a total analysis time of 120 minutes. The flow rate was passively split to 100 nL min^{-1} when performing the elution analysis. Nanospray was achieved using a distally coated fused silica emitter (New Objective, Cambridge, MA) (od 360 μm; id, 20 μm, tip id 10 μm) biased to 1.7 kV. A 33 MΩ resistor was introduced between the high voltage supply and the electrospray needle to reduce ion current.

The LTQ-Orbitrap mass spectrometer was operated in data-dependent mode, automatically switching between MS and MS/MS. Full scan MS spectra (300–1500 m/z) were acquired with a resolution of 60 000 at 400 m/z after accumulation to a target value of 500 000. The five most intense peaks above a threshold of 500 were selected for collision induced dissociation

in the linear ion trap at a normalized collision energy of 35 after accumulation to a target value of 30 000.

Data analysis

Raw MS-data were analyzed using Rosetta elucidator (http://www.rosettabio.com/products/elucidator), data management and analysis software capable of aligning mono-isotopic peaks of multiple LC-MS experiments. After grouping the data according to time point and fraction, the MS^1 peaks were aligned using the PeakTeller algorithm with a peak retention time window of 5 min. Subsequently, peak lists were generated by Rosetta elucidator and peptides were identified using the MASCOT v.2.2 search engine against the yeast SGD database (2008) containing 5779 entries (http://www.yeastgenome.org/). A mass tolerance of 0.6 Da was used for MS^2 data and a tolerance of 10 ppm was used for the MS^1 data.

Peptide identifications were selected with a minimum MASCOT ion score of 30. The 'visual script' feature of the Rosetta elucidator software was used to normalize the ^{14}N mono-isotopic MS^1 peptide peak intensities of each time point according to the sum of all peak intensities (^{14}N-labeled peptide peaks, $^{14}N/^{15}N$-labelled peptide peaks and ^{15}N-labelled peptide peaks). This was allowed, since the yeast biomass concentration was constant due to the constant growth rate. Subsequently, the identified ^{14}N peptides were grouped into proteins and their normalized ^{14}N mono-isotopic ion intensities were summed up. These normalized protein ^{14}N mono-isotopic peak intensities were used as input to calculate both the *S. cerevisiae* protein abundances and the corresponding turnover rates.

For each protein, a one-phase decay was fit by least squares using GraphPath Prism version 5.0 (http://www.graphpad.com/prism/Prism.htm). The plateau was constrained to be 0, and the rate constant to be ≥ 0. The data for each time point were weighted by the inverse of the measured variance (1/SD^2). All other settings were left at default values. From the output, the optimal decay rate K, its estimated standard error and R^2 of the fit were taken. Protein degradation rates and consequently half-lives could be calculated by subtracting the dilution rate of 0.1014 h^{-1} from the fitted K values. Only proteins with an R^2 value above 0.6 were kept in the final dataset.

Protein interaction networks were analyzed using the network analysis tool STRING.[23] The analysis was performed using the high confidence setting.

Conclusions

We present a mass spectrometry driven methodology to analyze wild type *S. cerevisiae* protein turnover rates under nitrogen limited conditions in a chemostat, by means of a pulse-chase-like approach. Combining this with label-free quantification enabled us to determine the abundance and degradation rates of 641 proteins. We show that, taken on average, protein turnover rates do not relate to protein abundance. Our data indicate that under nitrogen limitation, *S. cerevisiae* individual protein half-lives show a strikingly wide range of values, ranging from an estimated 30 min to over 20 h. We found that protein subunits involved in physical protein complexes, such as the ribosome, do exhibit turnover rates that are not necessarily in the same range, whereby complex functionality may be regulated by the protein with the shortest half-life. In pathways such as the glycolysis and TCA cycle, only a few proteins are very stable. We have shown that it is essential to study proteome characteristics like temporal dynamics and abundance on a large scale to add a new dimension to the systemic view of cellular processes.

Acknowledgements

This work was supported by the Netherlands Proteomics Centre and Kluyver Centre for Industrial Fermentation, both part of the Netherlands Genomics Initiative.

References

1 P. Picotti, B. Bodenmiller, L. N. Mueller, B. Domon and R. Aebersold, *Cell (Cambridge, Mass.)*, 2009, **138**, 795–806.
2 L. M. de Godoy, J. V. Olsen, J. Cox, M. L. Nielsen, N. C. Hubner, F. Frohlich, T. C. Walther and M. Mann, *Nature*, 2008, **455**, 1251–1254.
3 A. Kolkman, P. Daran-Lapujade, A. Fullaondo, M. M. Olsthoorn, J. T. Pronk, M. Slijper and A. J. Heck, *Mol. Syst. Biol.*, 2006, **2**, 2006 0026.
4 M. J. de Groot, P. Daran-Lapujade, B. van Breukelen, T. A. Knijnenburg, E. A. de Hulster, M. J. Reinders, J. T. Pronk, A. J. Heck and M. Slijper, *Microbiology (Reading, U. K.)*, 2007, **153**, 3864–3878.
5 S. P. Gygi, Y. Rochon, B. R. Franza and R. Aebersold, *Mol. Cell. Biol.*, 1999, **19**, 1720–1730.
6 M. W. Schmidt, A. Houseman, A. R. Ivanov and D. A. Wolf, *Mol. Syst. Biol.*, 2007, **3**, 79.
7 T. Rossignol, D. Kobi, L. Jacquet-Gutfreund and B. Blondin, *J. Appl. Microbiol.*, 2009, **107**, 47–55.
8 P. Daran-Lapujade, J. M. Daran, A. J. van Maris, J. H. de Winde and J. T. Pronk, *Adv. Microb. Physiol.*, 2009, **54**, 257–311.
9 B. J. Cargile, J. L. Bundy, A. M. Grunden and J. L. Stephenson, Jr., *Anal. Chem.*, 2004, **76**, 86–97.
10 P. K. Rao, G. M. Rodriguez, I. Smith and Q. Li, *Anal. Chem.*, 2008, **80**, 6860–6869.
11 J. M. Pratt, J. Petty, I. Riba-Garcia, D. H. Robertson, S. J. Gaskell, S. G. Oliver and R. J. Beynon, *Mol. Cell. Proteomics*, 2002, **1**, 579–591.
12 A. A. Cohen, N. Geva-Zatorsky, E. Eden, M. Frenkel-Morgenstern, I. Issaeva, A. Sigal, R. Milo, C. Cohen-Saidon, Y. Liron, Z. Kam, L. Cohen, T. Danon, N. Perzov and U. Alon, *Science*, 2008, **322**, 1511–1516.
13 M. K. Doherty, D. E. Hammond, M. J. Clague, S. J. Gaskell and R. J. Beynon, *J. Proteome Res.*, 2009, **8**, 104–112.
14 M. K. Doherty, C. Whitehead, H. McCormack, S. J. Gaskell and R. J. Beynon, *Proteomics*, 2005, **5**, 522–533.
15 A. Belle, A. Tanay, L. Bitincka, R. Shamir and E. K. O'Shea, *Proc. Natl. Acad. Sci. U. S. A.*, 2006, **103**, 13004–13009.
16 N. Gustavsson, B. Greber, T. Kreitler, H. Himmelbauer, H. Lehrach and J. Gobom, *Proteomics*, 2005, **5**, 3563–3570.
17 K. P. Jayapal, S. Sui, R. J. Philp, Y. J. Kok, M. G. Yap, T. J. Griffin and W. S. Hu, *J. Proteome Res.*, 2010, **9**, 2087–2097.
18 C. Vogel and E. M. Marcotte, *Nat. Protocols*, 2008, **3**, 1444–1451.
19 J. Malmstrom, M. Beck, A. Schmidt, V. Lange, E. W. Deutsch and R. Aebersold, *Nature*, 2009, **460**, 762–765.
20 J. C. Silva, M. V. Gorenstein, G. Z. Li, J. P. Vissers and S. J. Geromanos, *Mol. Cell. Proteomics*, 2006, **5**, 144–156.
21 M. E. Sardiu, Y. Cai, J. Jin, S. K. Swanson, R. C. Conaway, J. W. Conaway, L. Florens and M. P. Washburn, *Proc. Natl. Acad. Sci. U. S. A.*, 2008, **105**, 1454–1459.
22 B. Schwanhäusser, D. Busse, N. Li, G. Dittmar, J. Schuchhardt, J. Wolf, W. Chen and M. Selbach, *Nature*, 2011, **473**, 337–342.
23 L. J. Jensen, M. Kuhn, M. Stark, S. Chaffron, C. Creevey, J. Muller, T. Doerks, P. Julien, A. Roth, M. Simonovic, P. Bork and C. von Mering, *Nucleic Acids Res.*, 2009, **37**, 412–416.

24 A. J. Qavi, A. L. Washburn, J. Y. Byeon and R. C. Bailey, *Anal. Bioanal. Chem.*, 2009, **394**, 121–135.
25 R. Schiess, L. N. Mueller, A. Schmidt, M. Mueller, B. Wollscheid and R. Aebersold, *Mol. Cell. Proteomics*, 2009, **8**, 624–638.
26 H. Neubert, T. P. Bonnert, K. Rumpel, B. T. Hunt, E. S. Henle and I. T. James, *J. Proteome Res.*, 2008, **7**, 2270–2279.
27 V. M. Boer, J. H. de Winde, J. T. Pronk and M. D. Piper, *J. Biol. Chem.*, 2003, **278**, 3265–3274.
28 A. Kolkman, P. Daran-Lapujade, A. Fullaondo, M. M. A. Olsthoorn, J. T. Pronk, M. Slijper and A. J. R. Heck, *Mol. Syst. Biol.*, 2006, **2**, 1–16.
29 J. M. Pratt, J. Petty, I. Riba-Garcia, D. H. Robertson, S. J. Gaskell, S. G. Oliver and R. J. Beynon, *Mol. Cell. Proteomics*, 2002, **1**, 579–591.
30 A. Y. Dunn, M. W. Melville and J. Frydman, *J. Struct. Biol.*, 2001, **135**, 176–184.
31 C. Dekker, P. C. Stirling, E. A. McCormack, H. Filmore, A. Paul, R. L. Brost, M. Costanzo, C. Boone, M. R. Leroux and K. R. Willison, *EMBO J.*, 2008, **27**, 1827–1839.
32 R. J. Planta and W. H. Mager, *Yeast*, 1998, **14**, 471–477.
33 A. Verschoor, J. R. Warner, S. Srivastava, R. A. Grassucci and J. Frank, *Nucleic Acids Res.*, 1998, **26**, 655–661.
34 G. Kramer, D. Boehringer, N. Ban and B. Bukau, *Nat. Struct. Mol. Biol.*, 2009, **16**, 589–597.
35 T. Kruiswijk, R. J. Planta and W. H. Mager, *Eur. J. Biochem.*, 1978, **83**, 245–252.
36 P. P. Mueller, P. Grueter, A. G. Hinnebusch and H. Trachsel, *J. Biol. Chem.*, 1998, **273**, 32870–32877.
37 J. R. Warner and K. B. McIntosh, *Mol. Cell*, 2009, **34**, 3–11.
38 J. F. Dice and R. T. Schimke, *J. Biol. Chem.*, 1972, **247**, 98–111.
39 D. F. Nathan, M. H. Vos and S. Lindquist, *Proc. Natl. Acad. Sci. U. S. A.*, 1997, **94**, 12949–12956.
40 K. A. Borkovich, F. W. Farrelly, D. B. Finkelstein, J. Taulien and S. Lindquist, *Mol. Cell. Biol.*, 1989, **9**, 3919–3930.
41 M. G. Catlett and K. B. Kaplan, *J. Biol. Chem.*, 2006, **281**, 33739–33748.
42 P. K. Bansal, A. Nourse, R. Abdulle and K. Kitagawa, *J. Biol. Chem.*, 2009, **284**, 3586–3592.
43 T. R. Gemmill, X. Wu and S. D. Hanes, *J. Biol. Chem.*, 2005, **280**, 15510–15517.
44 M. Arevalo-Rodriguez and J. Heitman, *Eukaryotic Cell*, 2005, **4**, 17–29.
45 A. Matouschek, S. Rospert, K. Schmid, B. S. Glick and G. Schatz, *Proc. Natl. Acad. Sci. U. S. A.*, 1995, **92**, 6319–6323.
46 B. Bukau and A. L. Horwich, *Cell (Cambridge, Mass.)*, 1998, **92**, 351–366.
47 J. Becker and E. A. Craig, *Eur. J. Biochem.*, 1994, **219**, 11–23.
48 Z. Dragovic, S. A. Broadley, Y. Shomura, A. Bracher and F. U. Hartl, *EMBO J.*, 2006, **25**, 2519–2528.
49 J. P. Navarro-Avino, R. Prasad, V. J. Miralles, R. M. Benito and R. Serrano, *Yeast*, 1999, **15**, 829–842.
50 F. Saint-Prix, L. Bonquist and S. Dequin, *Microbiology (Reading, U. K.)*, 2004, **150**, 2209–2220.
51 J. M. Gancedo, *Microbiol. Mol. Biol. Rev.*, 1998, **62**, 334–361.
52 S. Ghaemmaghami, W. K. Huh, K. Bower, R. W. Howson, A. Belle, N. Dephoure, E. K. O'Shea and J. S. Weissman, *Nature*, 2003, **425**, 737–741.
53 R. Costenoble, P. Picotti, L. Reiter, R. Stallmach, M. Heinemann, U. Sauer and R. Aebersold, *Mol. Syst. Biol.*, 2011, **7**, 464.
54 J. M. Gancedo, D. Clifton and D. G. Fraenkel, *J. Biol. Chem.*, 1977, **252**, 4443–4444.
55 B. Przybyla-Zawislak, R. A. Dennis, S. O. Zakharkin and M. T. McCammon, *Eur. J. Biochem.*, 1998, **258**, 736–743.
56 M. Birney, H. Um and C. Klein, *Arch. Biochem. Biophys.*, 1997, **347**, 103–112.
57 S. L. Tai, P. Daran-Lapujade, M. A. Luttik, M. C. Walsh, J. A. Diderich, G. C. Krijger, W. M. van Gulik, J. T. Pronk and J. M. Daran, *J. Biol. Chem.*, 2007, **282**, 10243–10251.
58 M. L. Jansen, J. A. Diderich, M. Mashego, A. Hassane, J. H. de Winde, P. Daran-Lapujade and J. T. Pronk, *Microbiology (Reading, U. K.)*, 2005, **151**, 1657–1669.
59 C. Verduyn, E. Postma, W. A. Scheffers and J. P. Van Dijken, *Yeast*, 1992, **8**, 501–517.
60 M. A. van den Berg, P. de Jong-Gubbels, C. J. Kortland, J. P. van Dijken, J. T. Pronk and H. Y. Steensma, *J. Biol. Chem.*, 1996, **271**, 28953–28959.
61 A. Shevchenko, M. Wilm, O. Vorm and M. Mann, *Anal. Chem.*, 1996, **68**, 850–858.
62 S. Gauci, A. O. Helbig, M. Slijper, J. Krijgsveld, A. J. Heck and S. Mohammed, *Anal. Chem.*, 2009, **81**, 4493–4501.

